SCIENCE CHINA
Information Sciences

• **Supplementary File** •

Distributed Model-Free Adaptive Predictive Control of Traffic Lights for Multiple Interconnected Intersections

Xinfeng Ru[1], Chenyi Mei[1], Weiguo Xia[1*] & Peng Shi[2]

[1]*Key Laboratory of Intelligent Control and Optimization for Industrial Equipment of Ministry of Education, Dalian University of Technology, Dalian* 116024, *China;;*
[2]*School of Electrical and Electronic Engineering, The University of Adelaide, Adelaide SA 5005, Australia*

Appendix A Dynamics of Multiple Interconnected Intersections

In this article, the multi-intersection network is considered as a group of one-way road system. The multi-intersection network is divided into N interconnected subsystems, each of which is comprised of one intersection and two incoming links with traffic streams entering it. Each subsystem is a typical switching model since there are alternating red and green lights. We illustrate the model with a single-intersection example, as shown in Fig. A1. Let $\rho_a(k)$ and $\rho_b(k)$ represent the density of vehicles on roads a and b of subsystem i at discrete-time step k, respectively. We assume that all the intersections have the same cycle time T. Considering that the subsystem contains two links and two phases, it is easy to check that the dynamics of the traffic system can be presented as follows

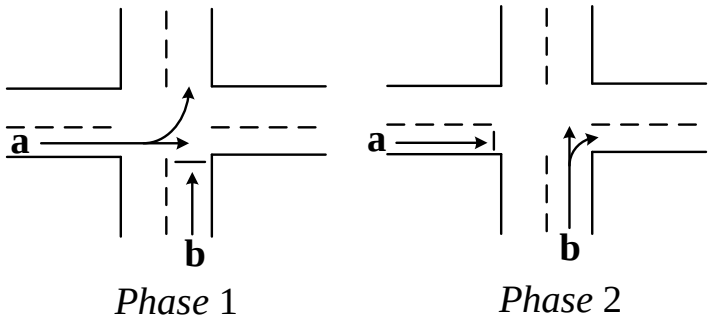

Figure A1 Two Phases for a single intersection.

Phase 1:

$$\begin{cases} \rho_a(k+t_1) = \rho_a(k) + \frac{1}{l_a}\left(q_a^1(k) - \alpha_a(k)u_{i1}(k)\right), \\ \rho_b(k+t_1) = \rho_b(k) + \frac{q_b^1(k)}{l_b}, \end{cases} \tag{A1}$$

Phase 2:

$$\begin{cases} \rho_a(k+1) = \rho_a(k+t_1) + \frac{q_a^2(k)}{l_a}, \\ \rho_b(k+1) = \rho_b(k+t_1) + \frac{1}{l_b}\left(q_b^2(k) - \alpha_b(k)u_{i2}(k)\right), \end{cases} \tag{A2}$$

where $u_{i1}(k)$ and $u_{i2}(k)$ are green times for *Phase* 1 and *Phase* 2, respectively. Let $\rho_a(k+t_1)$ and $\rho_b(k+t_1)$ denote the density of vehicles on roads a and b after *Phase* 1, respectively, l_a and l_b are the lengths of roads a and b, respectively, $q_a^1(k)$, $q_b^1(k)$ and $q_a^2(k)$, $q_b^2(k)$ represent the inflows of roads a and b in *Phase* 1 and *Phase* 2, respectively, and $\alpha_a(k)$ and $\alpha_b(k)$ denote the outflow rates of roads a and b, respectively. According to (A1)-(A2), a road facing a red light will see an increase of vehicle density due to the inflow of vehicles, whereas a road facing a green light will experience an outflow to the downstream roads.

Then, the dynamics of subsystem i can be rewritten as

$$y_i(k+1) = y_i(k) + z_i(k) - \beta_i(k)u_i(k), \tag{A3}$$

where $y_i(k) \triangleq [\rho_a(k), \rho_b(k)]^T$ denotes the density of vehicles of subsystems i; $z_i(k) \triangleq \left[\frac{q_a(k)}{l_a}, \frac{q_b(k)}{l_b}\right]^T$ is the interconnected influence from the neighboring subsystems, where $q_a(k) \triangleq q_a^1(k) + q_a^2(k)$, $q_b(k) = q_b^1(k) + q_b^2(k)$; $\beta_i(k) = diag\left[\frac{\alpha_a(k)}{l_a}, \frac{\alpha_b(k)}{l_b}\right]$ is a

* Corresponding author (email: wgxiaseu@dlut.edu.cn)

diagonal matrix denoting the vehicle density outflow rate of subsystem i; $u_i(k) = [u_{i1}(k), u_{i2}(k)]^T$ is the green time for subsystem i. The constraint condition of the control input for subsystem i is defined as follows

$$u_i^{\min} \leqslant u_i(k) \leqslant u_i^{\max}, \tag{A4}$$

$$u_{i1}(k) + u_{i2}(k) + L_i = T, \tag{A5}$$

where L_i is the yellow light time at subsystem i and keeps unchanged during the optimization process.

For all the subsystems $j \in \mathcal{N}_i$, let $z_{ji}(k)$ be the interconnected influence from subsystem j to subsystem i. For $j \notin \mathcal{N}_i$, one has $z_{ji}(k) = 0$. The physical meaning of $z_{ji}(k)$ is the increment of the density of vehicles contributed by subsystem j to subsystem i. Then, let the augmented control input vector be defined as

$$V_i(k) = \left[u_i^T(k), z_i^T(k)\right]^T,\ z_i(k) = \left[z_{j_1 i}(k), \ldots, z_{j_{|\mathcal{N}_i|} i}(k)\right]^T, \tag{A6}$$

where $z_i(k)$ is the interconnected influences. It should be noted that the augmented control input vector $V_i(k)$ constitutes of the control input $u_i(k)$ and the interconnected influences $z_i(k)$ from neighboring subsystems.

Then, the dynamics of subsystem i can be rewritten as, following from (A3) and (A6)

$$y_i(k+1) = f_i(y_i(k), V_i(k)). \tag{A7}$$

Appendix B Assumptions

Assumption 1. The partial derivative of $f_i(\cdot)$ in (1) with respect to each component of the control vector $V_i(k)$ is continuous.

Assumption 2. The generalized Lipschitz condition is met by each subsystem in (1), i.e., there exists a positive constant b_i, such that

$$|y_i(k_1+1) - y_i(k_2+1)| \leqslant b_i \left\|V_i(k_1) - V_i(k_2)\right\|, \tag{B1}$$

where $i = 1, \ldots, N$ and $V_i(k_1) \neq V_i(k_2)$, for any $k_1, k_2 > 0$.

It is easy to verify Assumption 1 for the urban traffic system based on the dynamics of the multi-interconnected subsystem (1), which is a common assumption while designing controllers for the nonlinear systems. Assumption 2, a physical restriction imposed by the fundamental characteristics of the urban traffic systems, means a finite change in vehicle flow does not result in an infinite change in the density of vehicles in a subsystem.

Appendix C Estimate of $A_i(k)$

The function $\phi_i(k)$ can be estimated and forecasted with the following cost function [1–3]

$$J(\phi_i(k)) = \left\|y_i(k) - y_i(k-1) - \phi_i^T(k)\Delta V_i(k-1)\right\|_2^2 + \mu_i \left\|\phi_i(k) - \hat{\phi}_i(k-1)\right\|_2^2, \tag{C1}$$

where $\hat{\phi}_i(k)$ is the estimate of $\phi_i(k)$, $\mu_i > 0$ is a weighting factor to restrain the exaggerated change of pseudogradients, and $\|x\|_2$ denotes the 2-norm of a vector x. The difference between the actual measured density of vehicles in subsystem i and the output of the CFDL data model is represented by the first term in (C1), while the second term punishes excessive variations of the pseudogradients. Then, the estimation of the pseudogradient $\hat{\phi}_i(k)$ can be updated by minimizing (C1) with respect to $\phi_i(k)$

$$\hat{\phi}_i(k) = \hat{\phi}_i(k-1) + \frac{\eta_i \Delta V_i(k-1)}{\mu_i + \|\Delta V_i(k-1)\|_2^2} \times \left[y_i(k) - y_i(k-1) - \hat{\phi}_i^T(k-1)\Delta V_i(k-1)\right], \tag{C2}$$

where $\eta_i \in (0, 1]$. Unfortunately, the CFDL data model cannot be used to get $\phi_i^T(k+1), \ldots, \phi_i^T(k+M-1)$ in $A_i(k)$ directly. A multi-layer hierarchical forecasting method is employed in this article to forecast these pseudogradients, and one has

$$\hat{\phi}_i(k+j) = \theta_1(k)\hat{\phi}_i(k+j-1) + \theta_2(k)\hat{\phi}_i(k+j-2) + \cdots + \theta_m(k)\hat{\phi}_i(k+j-m), \tag{C3}$$

where $j = 1, \ldots, M-1$ and m is an appropriate order and normally set as 2-7 [1, 4].

Then, let $\boldsymbol{\theta(k)} \triangleq [\theta_1(k), \ldots, \theta_m(k)]^T$, which can be updated according to the following equation

$$\boldsymbol{\theta(k)} = \boldsymbol{\theta(k-1)} + \frac{\hat{\Xi}_i^T(k-1)}{\delta + \left\|\hat{\Xi}_i(k-1)\right\|_2} \left[\hat{\phi}_i(k) - \hat{\Xi}_i(k-1)\boldsymbol{\theta(k-1)}\right], \tag{C4}$$

where $\hat{\Xi}_i(k-1) = \left[\hat{\phi}_i(k-1), \ldots, \hat{\phi}_i(k-m)\right]$, and $\delta \in (0, 1]$ is employed to avoid that the denominator equals to zero.

Appendix D The flow chart of the proposed DED-MFAPC scheme.

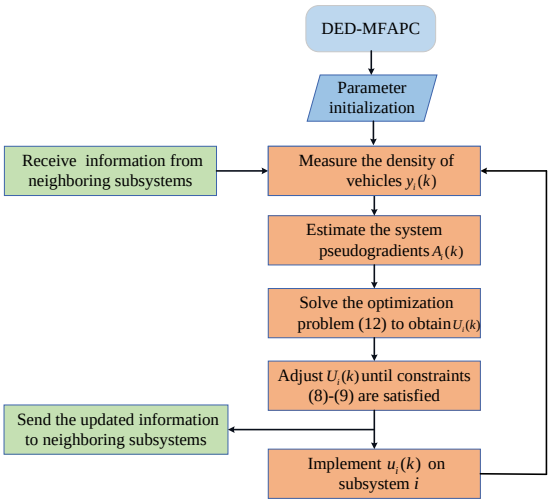

Figure D1 The flow chart of the proposed DED-MFAPC scheme.

Appendix E Case study

The DED-MFAPC scheme is proposed for traffic light control of multiple interconnected intersections aiming to generate balanced traffic distribution. In VISSIM simulation software, a 9-intersection topological network in Figure E1 is exploited to evaluate the validity of the proposed DED-MFAPC method. By contrasting the proposed DED-MFAPC approach with the fixed-time control (FTC), Bang-Bang control (BBC), and DED-MFAC methods [6], the effectiveness and nice performance of the proposed strategy is shown.

1) FTC indicates that each intersection uses the fixed signal timing scheme i.e., each phase accounts for half of the cycle time in this article.

2) According to the density of vehicles in each subsystem, BBC switches the maximum and minimum control input flowing out the subsystem, which is a common method in urban traffic control [5].

3) DED-MFAC strategy, a simplified version of the DED-MFAPC strategy, was employed in [6] to study the perimeter control of urban traffic networks.

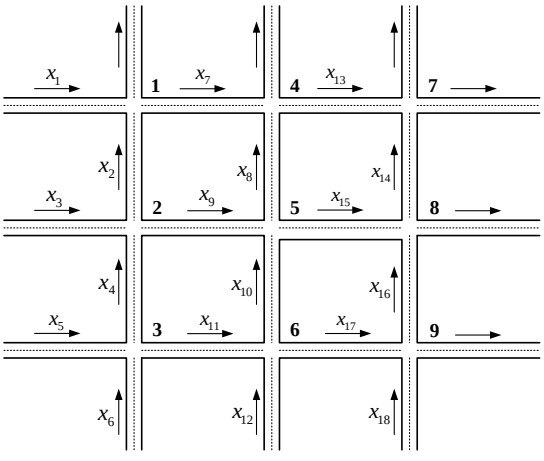

Figure E1 A 9-intersection network.

Table E1 displays the traffic demand for the experiment's scenarios that mimic the morning rush hour. As time goes on, the traffic demand of the network is gradually increasing. For each phase, the lower bound $u_i^{\min}$ and upper bound $u_i^{\max}$ are set as 20s and 40s, respectively. The cycle time of each intersection in the network is 60s. In addition, the prediction horizon is set to $M = 5$.

To compare the performance of the control strategies, with the traffic demand of the network in Table E1, three criteria, including the average density, the average flow rate, and the relative loss time, are compared. The average density is the average of the density of all vehicles on the roads, and a low average density indicates that there is generally less congestion and more throughput in the

Table E1 Traffic demand of the network.

Time step	0-20	20-60	60-130	130-200
demand(veh/h)	600	650	850	1050

network. In addition, the average flow rate implies the network's traffic situation through quantities such as the total delay time of vehicles, the average travel speed, the throughput of network and so on. The relative loss time means time lost per second by vehicles relative to free-flowing vehicles, which is an essential indicator to reveal the traffic congestion of the network. A thorough analysis of all the above criteria can be used to evaluate the traffic situation.

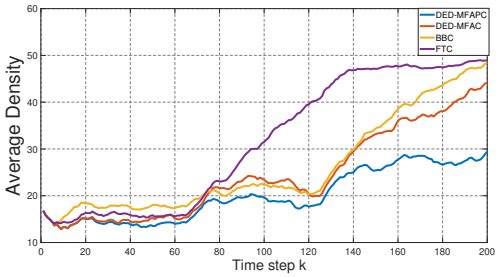

Figure E2 Comparison of the average density of vehicles on the roads under different control strategies.

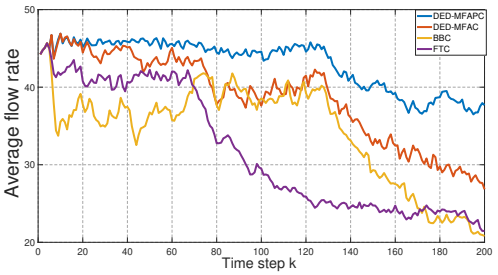

Figure E3 Comparison of the average flow rate under different control strategies.

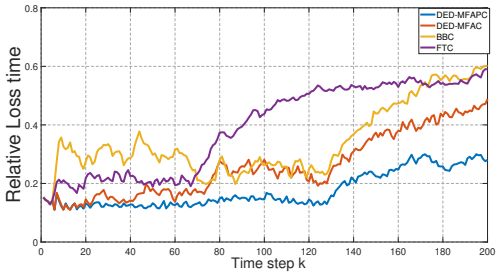

Figure E4 Comparison of the relative loss time under different control strategies.

The control performances of the various control strategies are compared in Figure E2-E4 and Table E2. Figure E2 displays the average vehicle density in the network for various control strategies during the simulation period. All the control methods get comparable performance under the low traffic demand situation at 0-80 steps. However, the proposed DED-MFAPC has better performance under the high traffic demand at 80-200 steps. Figure E3 depicts the evolution of the average flow rate of the network. The average flow rate of all the compared control strategies decreases to various degrees when the traffic demand rises, but the proposed DED-MFAPC is slightly reduced compared with other strategies, which means the network roads are not congested enough, although under high traffic demand. Figure E4 illustrates the progression of the relative loss time in which DED-MFAPC always has the best performance under all the compared control strategies. Figure E2-E4 show that the proposed DED-MFAPC performs better in the whole simulation process.

Table E2 The performance indexes under different control strategies

Control strategy	Average delay(s)	Average number of stops	Average speed(km/h)	Total travel time(h)
DED-MFAPC	119.671	3.010	42.567	3411.040
DED-MFAC	237.339	5.953	35.845	3974.367
BBC	286.162	6.443	33.640	4224.907
FTC	560.669	15.497	24.761	4835.764

To evaluate the effect of traffic light control more intuitively, four performance indexes include the average delay, average number of stops, average speed, and total travel time to evaluate various control methods, as indicated in Table E2. Those performance indexes can be obtained directly from VISSIM simulation software. Table E2 demonstrates that both DED-MFAC and BBC have better control effects than FTC, while DED-MFAPC has the best control effects because it has the largest average speed and the smallest average delay, average number of stops and total travel time.

References

1 Hou Z S, Chi R H, Gao H J. An overview of dynamic-linearization-based data-driven control and applications. IEEE Trans Ind Electron, 2016, 64: 4076-4090
2 Hou Z S, Xiong S S. On model-free adaptive control and its stability analysis. IEEE Trans Autom Control, 2019, 64: 4555-4569
3 Hou Z S, Jin S T. Model free adaptive control. CRC press Boca Raton, FL, 2013
4 Li D, De Schutter B. Distributed model-free adaptive predictive control for urban traffic networks. IEEE Trans Control Syst Technol, 2021, 30: 180-192
5 Aboudolas K, Geroliminis N. Perimeter and boundary flow control in multi-reservoir heterogeneous networks. Transport Res Part B, 2013, 55: 265-281
6 Lei T, Hou Z S, Ren Y. Data-driven model free adaptive perimeter control for multi-region urban traffic networks with route choice. IEEE Trans Intell Transport Syst, 2019, 21: 2894-2905